

Solvent Accessibility of the Thrombin-thrombomodulin Interface

Jeffrey G. Mandell¹, Abel Baerga-Ortiz¹, Satoko Akashi², Koji Takio² and Elizabeth A. Komives^{1*}

¹Department of Chemistry and Biochemistry, University of California, San Diego, La Jolla CA 92093-0359, USA

²Division of Biomolecular Characterization RIKEN 2-1 Hirosawa, Wako, Saitama 351-01, Japan

The kinetics of solvent accessibility at the protein-protein interface between thrombin and a fragment of thrombomodulin, TMEGF45, have been monitored by amide hydrogen/deuterium ($H/{}^2H$) exchange detected by MALDI-TOF mass spectrometry. The interaction is rapid and reversible, requiring development of theory and experimental methods to distinguish $H/{}^2H$ exchange due to solvent accessibility at the interface from $H/{}^2H$ exchange due to complex dissociation. Association and dissociation rate constants were measured by surface plasmon resonance and amide $H/{}^2H$ exchange rates were measured at different pH values and concentrations of TMEGF45. When essentially 100% of the thrombin was bound to TMEGF45, two segments of thrombin became completely solvent-inaccessible, as evidenced by the pH insensitivity of the amide $H/{}^2H$ exchange rates. These segments form part of anion-binding exosite I and contain the residues for which alanine substitution abolishes TM binding. Several other regions of thrombin showed slowing of amide exchange upon TMEGF45 binding, but the exchange remained pH-dependent, suggesting that these regions of thrombin were rendered only partially solvent-inaccessible by TMEGF45 binding. These partially inaccessible regions of thrombin form both surface and buried contacts into the active site of thrombin and contain residues implicated in allosteric changes in thrombin upon TM binding.

© 2001 Academic Press

Keywords: thrombin; amide $H/{}^2H$ exchange; anticoagulant; MALDI-TOF mass spectrometry; hydration

*Corresponding author

Introduction

Thrombomodulin (TM) binding to thrombin inhibits the fibrinogen cleavage activity of thrombin, and promotes thrombin cleavage and activation of protein C. In turn, protein C inactivates the essential cofactors required for the coagulation cascade, thus shutting down further production of thrombin (Esmon, 2000). TM has six EGF-like domains and the fifth domain contains most of the thrombin-binding residues. TMEGF45, containing both the fourth and fifth EGF-like domains, binds more tightly than the fifth domain alone, and is the smallest fragment capable of altering thrombin

activity. TMEGF456 has no additional cofactor activity but a tenfold smaller K_d (low nanomolar) than TMEGF45 (White *et al.*, 1995). Therefore, several TM domains play a role in altering the activity of thrombin. NMR experiments show at least two residues in the fourth domain, the three residues between the fourth and fifth domain, and nearly the entire fifth domain undergo chemical shift perturbations in the presence of thrombin (Wood *et al.*, 2000). The crystal structure of thrombin bound to TMEGF456 also shows a large interface of extensive contacts between thrombin and parts of all three EGF-like domains (Fuentes-Prior *et al.*, 2000).

In order to discover the essential parts of this large protein-protein interface, we chose to carry out amide hydrogen/deuterium ($H/{}^2H$) exchange experiments because they give solution phase solvent-accessibility information that cannot be gleaned from a static crystal structure. We recently reported the map of the surface of thrombin that becomes excluded from solvent upon TM binding,

Abbreviations used: TM, thrombomodulin; EGF, epidermal growth factor; MALDI-TOF, matrix-assisted laser desorption/ionization time-of-flight; MS, mass spectrometry; $H/{}^2H$, hydrogen/deuterium.

E-mail address of the corresponding author: ekomives@ucsd.edu

which includes anion-binding exosite 1 and regions near the active site (Mandell *et al.*, 1998b). In that study, it was not possible to distinguish amides that were completely solvent-excluded from those that were only partly excluded at the interface. Computational studies have indicated that both types of amides are found at protein-protein interfaces and that 67% of the interface is only partially solvent-excluded (Lo Conte *et al.*, 1999). Alanine scanning experiments have also shown that only a few of the residues in contact in the protein-protein interface actually determine the thermodynamic stability of the interaction, and these were termed the "hot spot" of the interaction (Cunningham & Wells, 1993; Wells, 1996).

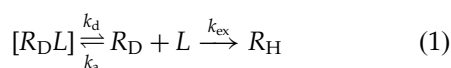
We hypothesized that the thermodynamically important part of the interface may be the solvent-excluded part. Experiments were designed to find these completely solvent-excluded regions within the interface by a thorough kinetic analysis of H/²H exchange rates at the interface. A key component of the experiment was to measure the pH-dependence of the exchange rates, knowing that near physiological pH, the intrinsic exchange rate is log-linear with [OH⁻] (Hvidt & Nielson, 1966). The rates of exchange of completely solvent-excluded amides should be less pH-dependent than the exchange rates of partially solvent-accessible amides because they can only exchange while the complex is dissociated.

We present results that show that two segments of thrombin contain completely solvent-excluded amides when TMEGF45 is bound, and several other segments show partial solvent exclusion. The completely solvent-excluded segments map to anion-binding exosite 1 and contain a tyrosine residue for which mutation to alanine abolishes binding (Hall *et al.*, 1999). The other regions show exchange rates that are pH dependent, and therefore retain partial solvent accessibility. One of these regions helps form the back side of the active site of thrombin. Three other regions are surface segments that form a pathway from anion-binding exosite 1 to the active site. These results provide a plausible explanation for the observed allosteric effects of TM on thrombin activity (Ye *et al.*, 1991). To our knowledge, this is the first report of an experimental measurement of the kinetics of solvent accessibility at a protein-protein interface.

Theory

Amide H/²H exchange rates at solvent-excluded protein-protein interfaces

For amides at a completely solvent-excluded protein-protein interface, the observed H/²H exchange rate is controlled by the protein-protein dissociation and association rates as well as the intrinsic rate of hydrogen exchange (k_{ex}):



Where R_H is protonated receptor, R_D is deuterated receptor, L is ligand, k_{ex} is the intrinsic amide exchange rate (min^{-1}) for amides in the uncomplexed receptor, k_d is the rate of dissociation of the complex (min^{-1}), and k_a is the rate of association of the proteins undergoing complexation ($\text{M}^{-1} \text{min}^{-1}$). It is important to note that k_{ex} is strongly pH-dependent, and near physiological pH is logarithmically dependent on [OH⁻]. The observed rate of exchange, k_{obs} , depends on the interplay between the kinetics of both complexation and H/²H exchange.

H/²H exchange at a protein-protein interface could occur because of solvent accessibility at the interface or because of exchange that occurs when the complex dissociates. Therefore, to measure only the solvent accessibility at the interface, it is important to carry out the experiment under conditions in which essentially 100% of the receptor is bound to ligand. The final protein concentration required for MALDI H/²H exchange measurement, is 3 μM , considerably above the K_d for most interactions, and therefore:

$$\% \text{ Bound} = \frac{L + R + K_d \pm \sqrt{(L + R + K_d)^2 - 4LR}}{2R}$$

If the K_d is less than 1 nM, a 1:1 ratio of ligand to receptor is sufficient to keep essentially 100% of the receptor bound throughout the experiment regardless of the complexation kinetics. If the K_d is 10-100 nM, then higher ratios of ligand to receptor are required to study H/²H exchange kinetics at the interface in the bound complex (Figure 1) and the interplay between the binding kinetics and exchange kinetics becomes important.

For the interactions with slow k_d values, i.e. less than 10^{-2} min^{-1} , the lifetime of the complex is hours, and it essentially never dissociates during a typical one hour experiment. For these complexes, the observed rate of H/²H exchange of amides that are completely solvent-excluded at the interface will simply equal k_d :

$$k_{\text{obs}} = k_d \quad \text{and} \quad k_d \approx 0 \quad (2)$$

Many protein-protein interactions have k_d values faster than 10^{-2} min^{-1} , and the complex will dissociate during the experiment. In these cases, it is necessary to consider the interplay between k_a , k_d , and the intrinsic H/²H exchange rate, k_{ex} :

$$k_{\text{obs}} = \frac{k_d k_{\text{ex}}}{k_a [\text{ligand}] + k_{\text{ex}}} \quad (3)$$

A quantitative estimate of k_{obs} is difficult to obtain because measured values of k_a vary from 10^6 - $10^9 \text{ M}^{-1} \text{ min}^{-1}$ and k_d can be as high as 10 min^{-1} (Wu *et al.*, 1996; Myszkka *et al.*, 1996). Experiments show that values of k_{ex} also vary considerably. The rates predicted by Bai *et al.* (1993)

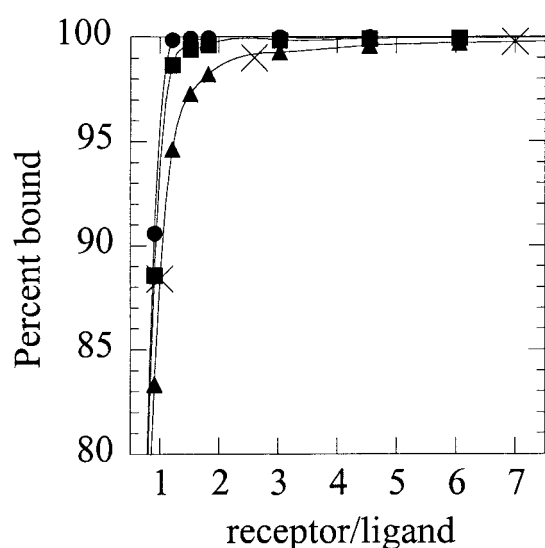


Figure 1. Plot of the relationship between the concentration of ligand, and the percentage of receptor that is bound in the experiment. Theoretical curves for $K_d = 0.1$ nM and 1 nM were essentially indistinguishable (●). To achieve 100% bound, receptor:ligand ratios greater than 1:1 are required for $K_d = 10$ nM (■) and higher. The curve for $K_d = 50$ nM (▲) shows that for these weaker binding affinities, ratios greater than 5:1 are required to achieve 100% bound. Actual experimental conditions for the thrombin-TMEGF45 interaction, which has a K_d close to 50 nM, are plotted on this curve for thrombin:TMEGF45 ratios of 1:1, 2.6:1 and 7:1 (X).

for unstructured polyalanine at 20°C are 360 min⁻¹ (pH 6.5), 3500 min⁻¹ (pH 7.5), and 8900 min⁻¹ (pH 7.9). However, the rates observed for surface amides in proteins are typically much less than the free exchange rates in unstructured peptides (Dharmasiri & Smith, 1996). At pH 7.5, these rates typically range from about 16 min⁻¹ to 570 min⁻¹ with a median of 30 min⁻¹ in the mannose permease domain P13 from *Escherichia coli* (Gemmecker *et al.*, 1993).

When K_d is higher than 10 nM, inevitably k_d will be fast enough that the complex will dissociate during the experiment. Figure 1 shows that for these cases, an excess of ligand will be required to achieve 100% bound, and we can define a pseudo first order rate constant ($k_a[\text{ligand}]$) that allows direct comparison of the terms in the denominator of equation (3). Many protein-protein interactions are expected to have $k_a[\text{ligand}] \approx k_{ex}$. In these cases, k_{obs} will depend on k_a , k_d and k_{ex} . We have studied one such example, the interaction between protein kinase A and its inhibitor, PKI, for which the kinetic constants are $k_d = 4.6 \times 10^{-2}$ min⁻¹, $k_a = 9 \times 10^7$ M⁻¹ min⁻¹, so $k_a[\text{ligand}] = 270$ min⁻¹ at the experimental concentration of 3 μM (Herberg *et al.*, 1999; J.G.M. *et al.*, unpublished data). In these cases, a full study of the relationship

between ligand concentration and k_{obs} will be necessary because values of k_{ex} vary widely.

Some protein-protein interactions such as thrombin-TMEGF45 ($K_d = 50$ nM) are in rapid equilibrium. In order to achieve 100% bound, a seven-fold excess of TMEGF45 was used resulting in $k_a[\text{ligand}] = 30,000$ min⁻¹ and the complex reassociates before an H/²H exchange event can take place regardless of the estimated value of k_{ex} . For these cases, equation (3) simplifies to:

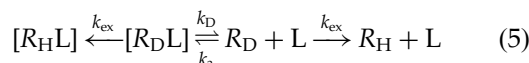
$$k_{obs} = \frac{K_d \cdot k_{ex}}{[\text{ligand}]} \quad (4)$$

High ratios of ligand to receptor ensure that k_{obs} reflects exchange at the interface and not exchange due to complex dissociation.

Dependence of amide exchange rate on pH as a criterion for solvent accessibility at the interface

The preceding discussion forms the framework for understanding the pH dependence of the observed exchange rates of completely solvent-excluded amides at protein-protein interfaces. For interactions where k_d is slow, $k_{obs} \approx 0$ and not pH-dependent. For protein-protein interactions that are in rapid equilibrium, k_{obs} will be a function of k_{ex} as well as K_d and ligand concentration (equation (4)). In these cases, the pH dependence of k_{obs} should be slight if the conditions of 100% bound are met by adding an excess of ligand.

All of the above discussion pertains only to amides that are completely solvent-excluded at the protein-protein interface. We can also consider the exchange rate of those amides that remain partly solvent-accessible at the interface. Interfaces are expected to contain a high percentage of such partly excluded amides (Lo Conte *et al.*, 1999). The exchange rates for these amides will depend on how solvent-inaccessible they are, and will vary from a lower limit of k_{obs} for completely solvent-inaccessible amides (Equation 3) up to a maximum value of the intrinsic exchange rate, k_{ex} (equation (5)):



Again, the solvent accessibility determines the degree to which the k_{obs} is pH dependent. The less solvent-accessible the amide is, the weaker the pH dependence will be. Conversely, the closer the exchange rate is to k_{ex} , the stronger the pH dependence will be. In all cases, it will be possible to differentiate amides that are partly solvent-accessible from those that are completely excluded from solvent at the interface by ascertaining the degree to which the observed H/²H exchange rate is pH dependent.

Results

Fragmentation of thrombin by pepsin

Cleavage of thrombin with pepsin resulted in about 35 peptides, of which 25 were identified (Figure 2). These peptides covered 50% of the thrombin sequence and 60% of the solvent-accessible surface. Regions of thrombin that contained disulfide bonds did not yield observable fragments. Electrospray ionization instead of MALDI did not result in significantly greater coverage, suggesting that sequence coverage was limited by disulfide bonding and not by the method of peptide ionization. It was not always possible to obtain quantitative data on each peptide for various reasons including weak signals and overlapping peaks. Quantitative data were obtained from 17 peptides that covered 48% of the thrombin sequence.

Determination of the thrombin-TMEGF45 binding kinetics

In order to understand the interplay between H/²H exchange and complexation kinetics, it was essential to determine the binding kinetic rate constants. The thrombin-TMEGF456 interaction is rapid and reversible with a k_a near $10^9 \text{ M}^{-1} \text{ min}^{-1}$ and a k_d near 2 min^{-1} (Baerga-Ortiz *et al.*, 2000). The K_d for TMEGF45 is 50 nM, roughly 20-fold

larger than for TMEGF456. TMEGF45 has a higher k_d compared with TMEGF456, which accounts for the difference in K_d . The binding kinetics of thrombin to TMEGF45 did not vary over the pH range used for the H/²H exchange experiments (Table 1).

Determination of TMEGF45 concentration required for H/²H exchange experiments

We observed increasing amounts of deuterium retained at the interface as the ratio of TMEGF45 to thrombin was increased from 2.6:1 to 7:1, corresponding to 98.77 and 99.78% bound, respectively (Figure 1). For the 2.6:1 ratio, the complex was apart for 1.5 seconds during two minutes of off-exchange time, and this was enough to decrease the observed deuteration compared with the 0.3 second apart at a 7:1 ratio. To ensure the observed H/²H exchange was for amides at the interface of the protein complex, and not due to complex dissociation, a ratio of TMEGF45 to thrombin of 7:1 was used for the quantitative measurement of exchange rates. At this ratio, the concentration of TMEGF45 was 24 μM and $k_a[\text{TM}] = 30,000 \text{ min}^{-1} \gg k_{ex}$. The possibility of non-specific binding arises with high ratios of ligand:receptor, so comparisons were made with lower ratios of TMEGF45:thrombin (data not shown). The same surface regions of thrombin showed slowed exchange in the complex at ratios of 7:1 and

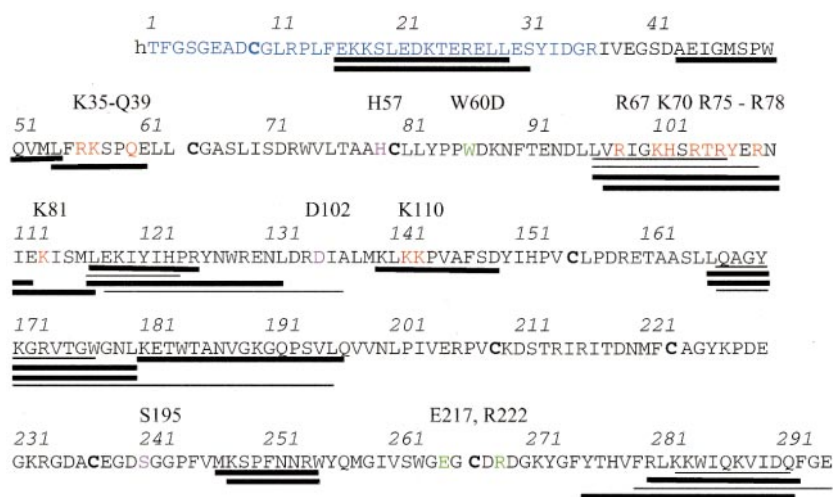


Figure 2. Sequence of human α -thrombin showing the peptides that were generated by pepsin cleavage and observed in a single MALDI-TOF mass spectrum. The light chain is indicated by blue text, the residues important for thrombin binding are colored red, the residues important for protein C activation are colored green, and the catalytic triad residues are colored purple. Peptides that resulted from cleavage of thrombin by pepsin are shown as lines below the sequence with thick lines representing peptides from which quantitative data were obtained, and thin lines representing peptides that were observed but not quantified. For non-quantifiable peptides differing by only a single residue, only one line is shown. The peptides covered 50% of the thrombin sequence and 60% of the solvent-accessible surface. The cysteine residues that form the disulfide bonds between C9 and C155, between C64 and C80, between C209 and C223, and between C237 and C267 are shown in bold letters. The disulfide bonds were not reduced, and coverage near the disulfide bonds was poor. Above the sequence, key residues are indicated in the commonly used chymotrypsin numbering scheme, but the sequential numbering scheme is used throughout the text for simplicity. Hall *et al.* (1999) use a third numbering scheme, which is sequential starting at residues in the heavy chain, so residues reported by Hall *et al.* (1999) are 36 less than the sequential numbers given here.

Table 1. The k_a , k_d and K_d of TMEGF45 as a function of pH

pH	k_a ($M^{-1} \text{ min}^{-1}$) $\times 10^8$	k_d (min^{-1})	K_d (nM)	% bound
6.5	3.6(± 0.5)	18.6(± 0.2)	52(± 13)	99.75
7.0	3.7(± 0.5)	18.6(± 0.2)	50(± 13)	99.76
7.5	4.0(± 0.5)	24.0(± 0.3)	60(± 15)	99.71
8.0	4.3(± 0.6)	22.2(± 0.3)	52(± 13)	99.75

The percentage of thrombin bound was calculated by assuming a [thrombin] of 3.3 μM and [TMEGF45] of 24 μM according to the following equation:

$$\% \text{ Bound} = \frac{L + R + K_d \pm \sqrt{(L + R + K_d)^2 - 4LR}}{2R}$$

2.6:1, consistent with a lack of non-specific binding.

Regions of thrombin that showed decreased H²H exchange rates upon complexation with TMEGF45

Initially, the rates of amide deuteration in free thrombin were determined as a measure of surface accessibility (Mandell *et al.*, 1998a). Rates of deuteration that were much slower than the mean value of 30 min^{-1} were taken as an indication that the region of thrombin might not be completely solvent-accessible. Caution was used in interpreting results from these regions, because changes in these regions might be due to secondary conformational changes. Kinetics of incorporation of deuterium into amide positions in each region of thrombin were measured in the absence of TMEGF45 at both pH 6.6 and 7.9. The rate of incorporation of deuterium at pH 7.9 is approximately 20-fold faster than at pH 6.6. On occasion, we observed more deuterium incorporation at pH 7.9 than at 6.6, indicating that some of the amides in the region exchanged slowly, and were therefore not completely deuterated after ten minutes at pH of 6.6. Based on the difference between the deuteration at pH 6.6 *versus* 7.9, the regions of thrombin presented here could be classified into three categories. Surface loop regions of thrombin incorporated deuterium rapidly at both pH values. Other regions spanned surface as well as partly buried sites. These showed rapid deuteration at pH 7.9, but also contained a few amides that became deuterated more slowly at pH 6.6 indicating that the region was not completely solvent-accessible. Finally, some regions incorporated deuterium slowly at both pH values. In the structure of thrombin, these regions had the least surface solvent-accessibility as determined by calculating the solvent-accessible surface area of each individual region using GRASP (Nicholls *et al.*, 1991).

In order to determine which regions of thrombin showed altered solvent-accessibility upon TMEGF45 binding, off-exchange experiments were performed. For these experiments, proteins were incubated in deuterated buffer of pH 6.6 or 7.9 for eight minutes, mixed together for two minutes

and then diluted tenfold into H₂O to initiate off-exchange. After varying lengths of time, the reaction was quenched to stop exchange, the thrombin was digested and the entire mixture of peptides was analyzed by mass spectrometry. Kinetic rates of off-exchange in the presence and absence of TMEGF45 were obtained from measurements over 30 minutes. Complete data from all 17 peptides were quantitatively analyzed for rates of deuterium incorporation and for rates of off-exchange of deuterium from amide positions.

Nine peptides representing six different regions of thrombin showed slowed off-exchange when thrombin was complexed with TMEGF45. These six different regions cover a large surface of the thrombin molecule (Figure 3). Complete analysis of data from all 17 peptides showed that the regions that did not change were scattered throughout the thrombin molecule while the surface that decreased solvent-accessibility is contiguous (Figure 3). Data for one region that did not change (residues 248 to 255, a surface loop) are presented in Figure 4. Mass spectra for the peptide corresponding to this region (m/z 1048.53) are shown in Figure 4(a). Kinetic data for incorporation of deuterium into this region are shown in Figure 4(b). Exchange of these deuterons back to protons in the presence and absence of TMEGF45 at pH 6.6 is plotted in Figure 4(c) and at pH 7.9 is plotted in Figure 4(d).

Solvent exclusion at anion-binding exosite I

Kinetics of deuterium incorporation into anion-binding exosite I were studied in two overlapping peptides spanning residues 96 to 112, (m/z 2127.19) and residues 97 to 117 (m/z 2586.44) (Figure 5(a) and (b)). The region is highly solvent-accessible with a percentage deuterium incorporated that was equivalent to values obtained previously for a completely unstructured peptide (Mandell *et al.*, 1998a). Deuterium incorporation was equivalently high at both pH values and both regions were fully deuterated by ten minutes (Table 2, Figure 5(b)). In the absence of TMEGF45, all amides in the region spanning residues 96 to 112 rapidly exchanged back to the value expected for a 1:10 dilution. When TMEGF45 was present,

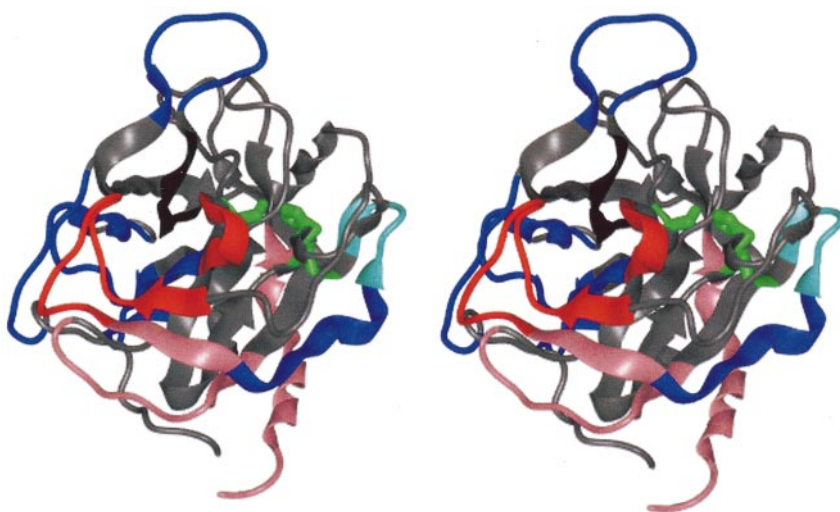


Figure 3. Stereo view of human α -thrombin showing the regions that had slowed amide hydrogen exchange in the complex with TMEGF45. The residues of the catalytic triad are in space-filling models and colored green. The regions that were not quantitatively covered are grey, and those that were covered but did not change upon TMEGF45 binding are blue. The two regions (residues 54 to 61 and 96 to 112) that were totally solvent-excluded in anion-binding exosite I are colored red. The region that forms the back side of the active site and is likely an allosteric change is colored black (residues 167 to 180). The regions that form a partially solvent-excluded path to the active site (residues 112

to 117, 139 to 149 and 281 to 293) are colored pink and the loop that is contacted by the C-terminal helix causing yet another allosteric change near the active site is cyan (residues 125 to 132).

three deuterons remained bound to thrombin even at long off-exchange at either pH (Table 2; Figure 5(c) and (d)). Another two deuterons exchanged slowly at pH 6.6 but quickly at pH 7.9 indicating that they remain partially solvent-accessible.

The longer peptide spanning residues 97 to 117 (m/z 2586.44) offered an opportunity to separately investigate residues 96 to 112 and 113 to 117. Nearly 11 amides within residues 97 to 117 were slowed to exchange in the presence of TMEGF45 (Figure 5(e)). Three of these amides remained deuterated in the complex even after very long times of off-exchange even at pH 7.9 (Figure 5(e) and (f)). These amides can be assigned to the 96-112 region of this peptide, since they were also observed in the shorter peptide (Table 2). The other eight amides that are slowed in this segment upon TMEGF45 binding remain partly solvent-accessible, based on comparisons of the data at pH 6.6 *versus* 7.9. Since only four amides were slowed in the 96-112 segment, the additional four slow amides observed in the 96-117 fragment can be assigned to the 113-117 region. Thus, nearly all of anion-binding exosite I is partially solvent excluded when TMEGF45 binds to thrombin. A core of three amides within the 96-112 regions remains completely solvent-excluded at the interface, while several more amides both in residues 96 to 112 and in residues 113 to 117, are partially solvent-excluded.

Solvent accessibility changes at an adjacent segment in anion binding exosite I

Residues 54 to 61 (peptide m/z 1004.55) form a surface-exposed loop on the edge of the active-site canyon near anion-binding exosite I (Figure 3). For this region, deuterium incorporation was slower at

pH 6.6 than at pH 7.9, indicating that it was less solvent-accessible (Table 3A). A higher level of deuterium incorporation was obtained at pH 7.9, and the extra deuterons exchanged back rapidly in both the presence and absence of TMEGF45. At both pH values in the presence of TMEGF45, 0.7-1.0 amide retained deuterium for very long times. The exchange rate of this amide did not vary with pH, so we can conclude that it is completely solvent-inaccessible in the complex.

A buried segment of thrombin containing Trp177 (Trp141 in the chymotrypsin numbering scheme) that interacts with Arg104 in anion-binding exosite 1 also showed slowing of amide H/ 2 H exchange in the presence of TMEGF45. This region was represented by two peptides spanning residues 167 to 180 (m/z 1506.78), and residues 166 to 180 (m/z 1619.87). The overlapping peptides gave identical results and data are only presented for residues 167 to 180 (Table 3B). Consistent with its buried character, this region was not very solvent-accessible as assessed from the extra four deuterons incorporated at pH 7.9 compared to pH 6.6. At pH 7.9 in the presence of TMEGF45 a significant slowing of amide off-exchange was observed for this region, but at pH 6.6 no significant slowing was observed. The most likely explanation for these data is that the amides that were slow to off-exchange in the complex only became deuterated at pH 7.9. The lower solvent-accessibility and partial solvent-inaccessibility in the complex is suggestive of allosteric or conformational changes upon TMEGF45 binding.

A surface path to the active site

Residues 139 to 149 (peptide m/z 1263.71) form a surface-exposed strand that lies between anion-binding exosite I and the C-terminal helix

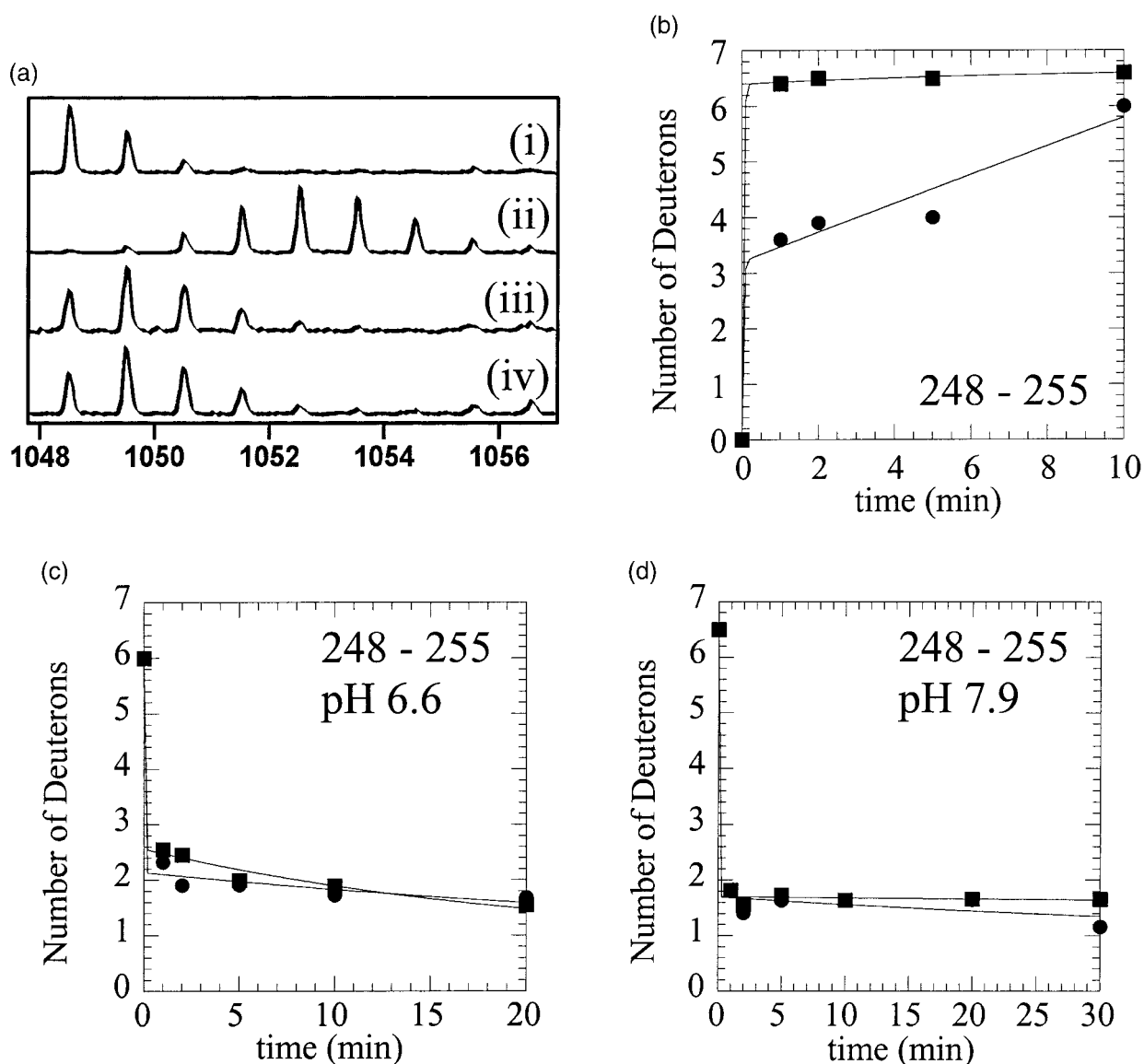


Figure 4. (a) Mass spectra of the peptide corresponding to the surface loop that did not change upon TMEGF45 binding (residues 248 to 255, m/z 1048.53) from the peptic digest of thrombin: (i) before deuteration; (ii) at ten minutes deuteration; (iii) after off-exchange in the absence of TMEGF45; and (iv) after off-exchange in the presence of TMEGF45. (b) Kinetics of deuterium incorporation into residues 248 to 255 at pH 6.6 (●) and pH 7.9 (■). (c) Kinetics of off-exchange of deuterium from residues 248 to 255 of thrombin at pH 6.6 alone (■) or in complex with TMEGF45 (●). (d) Kinetics of off-exchange of deuterium from residues 248 to 255 of thrombin at pH 7.9 alone (■) or in complex with TMEGF45 (●). The off-exchange experiments were done by dilution, and a residual amount of deuterium, proportional to the number of exchangeable sites, is still present on each peptide at infinite time.

(Figure 3). This region was fairly solvent-accessible (Table 4A). At pH 6.6 in the presence of TMEGF45, an average of 1.8 amides showed slowed exchange. At pH 7.9, no significant slowing of amide exchange was observed in this region, suggesting that this part of the interface is not completely solvent-excluded.

The C-terminal helix is adjacent to the 139 to 149 segment on the surface of thrombin. Two overlapping peptides, residues 276 to 292 (m/z 2202.25), and residues 281 to 293 (m/z 1702.02) correspond to this helix, and both showed slowing of amide exchange upon TMEGF45 binding (Figure 3). This

region contained amides that were solvent accessible and some that were less so, as assessed from the difference between deuterium incorporation at pH 6.6 compared to pH 7.9 (Table 4B, Figure 6(a)). At pH 6.6, all of the amides became less solvent-accessible and exchanged at an intermediate rate when TMEGF45 was bound (Figure 6(b)). At pH 7.9 when TMEGF45 was bound, two amides exchanged at a very slow rate (Figure 6(c)). One explanation for these observations is that the helix is tightening up upon TMEGF45 binding and all of the amides exchange somewhat more slowly. At pH 7.9, even those amides that incorporated

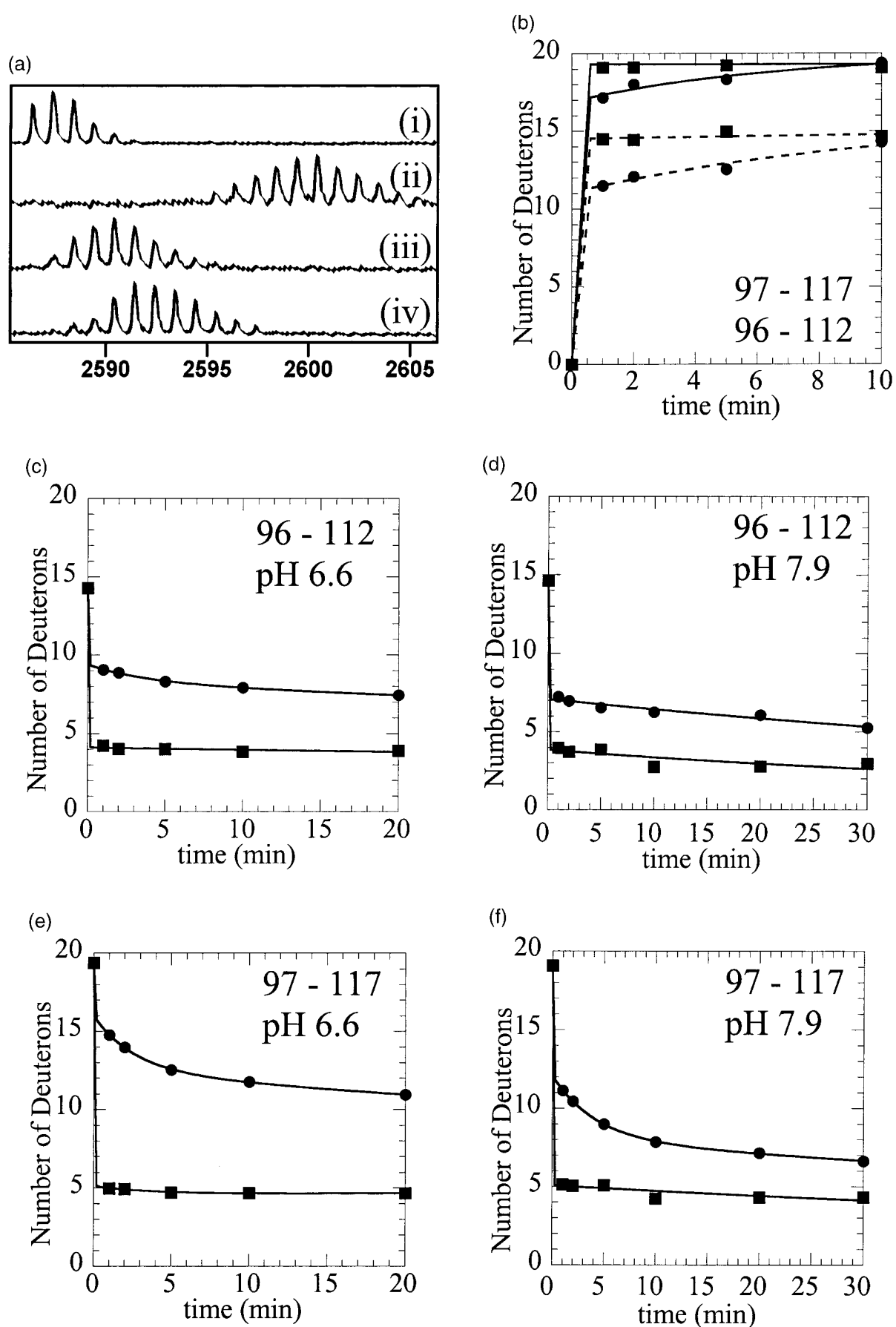


Figure 5 (legend opposite)

Table 2. Solvent accessibility of anion-binding exosite I

A. Sequence		Mass (MH+)			
96-112		2127.19			
Sample	On by 10 min (18.4 possible) ^a	Fast off (16 amides) ^b	Intermed off	Slow off	
pH 6.60 thrombin +TMEGF45	14.6	10.2 (0.15)	0	3.0 (0.08)	
pH 7.90 thrombin +TMEGF45	14.6	4.9 (0.15)	1.1 (0.32)	7.2 (0.40)	
		10.8 (0.50)	0	2.8 (0.28)	
		7.5 (0.23)	0	6.0 (0.13)	
B. Sequence		Mass (MH+)			
97-117		2586.44			
Sample	On by 10 min (22.8 possible) ^a	Fast off (20 amides) ^b	Intermed off	Slow off	
pH 6.60 thrombin +TMEGF45	19.4	14.3 (0.15)	0.5 (0.25)	3.4 (0.32)	
pH 7.90 thrombin +TMEGF45	19.2	3.4 (0.25)	3.6 (0.23)	11.2 (0.29)	
		14.1 (0.38)	0	3.8 (0.20)	
		7.0(0.12)	4.0 (0.17)	6.8 (0.22)	

All deuterium levels were corrected to account for ~40% loss during analysis.

The error to the fit for each value is indicated in parentheses.

^a The number of possible sites of deuteration = number of amides + 4.4% of all exchangeable sites (based on final dilution of sample before drying).

^b The number of backbone amides (not including the N-terminal residue).

deuterium more slowly became labeled, and these exchanged back at a slow rate when TMEGF45 was bound.

The C-terminal helix is adjacent to a loop near the edge of the active site that contains the catalytic aspartate. Two overlapping peptides spanning residues 117 to 125 (m/z 1168.68) and residues 117 to 132 (m/z 2144.14) enabled us to dissect this region, which was completely solvent-accessible, as evidenced by the same number of deuterons incorporated at both pH 6.6 and 7.9 (Table 4C and D). At both pH values, slowed exchange was observed when TMEGF45 was bound, but only for the 117-132 fragment, not for the 117-125 fragment. The exchange slowed only to an intermediate rate, indicating that the region remains partly solvent-accessible. Another fragment, spanning residues 117 to 126, could not be quantified due to overlap with another peak in the mass spectrum, but a small degree of solvent exclusion was apparent in the mass spectrum at both pH values. Since this peptide overlaps with 117-125 (which showed identical H/²H exchange kinetics in the presence and absence of TMEGF45), the amide that slows upon TMEGF45 binding can be attributed to Tyr126. This residue is within 2.5 Å of catalytic Asp135. Finally, a peptide spanning residues 118 to 136 also showed qualitatively the same increase in mass as was seen for residues 117 to 132.

Discussion

Correlation between solvent exclusion and the "hot spot" of the interaction

Three amides within residues 96 to 112 became completely solvent-inaccessible upon TMEGF45 binding. This segment contains Tyr107 (Tyr71 in the work by Hall *et al.*, 1999), which when mutated to alanine shows a large decrease in TM binding (Hall *et al.*, 1999). We also observed one solvent-inaccessible amide in the segment containing residues 54 to 61. This segment forms the edge of anion-binding exosite I, and contains Leu54 and Phe55, which appear to form a hydrophobic pocket for binding Ile414 of TM in the crystal structure of the thrombin-TMEGF456 complex (Fuentes-Prior *et al.*, 2000).

Wells' group has coined the term for those few sites in a protein-protein interface at which alanine mutations abolish binding as the hot spot of the interaction. In human growth hormone, the hot spot was a small region of the entire interface observed in the crystal structure of the complex. The hot spot residues determine the thermodynamic stability of the protein-protein complex (Wells, 1996). Our results suggest that the solvent-inaccessible core of the interface corresponds to the hot spot. In other words, the region that is completely solvent-inaccessible seems to correspond to the

Figure 5. (a) Mass spectra of the peptide corresponding to anion-binding exosite I (residues 97 to 117 m/z 2586.44) from the peptic digest of thrombin: (i) before deuteration; (ii) at ten minutes deuteration; (iii) after off-exchange in the absence of TMEGF45; and (iv) after off-exchange in the presence of TMEGF45. (b) Kinetics of deuterium incorporation into amides of thrombin at pH 6.6 (●) and pH 7.9 (■) residues 97 to 117 (continuous lines) and residues 96 to 112 (broken lines). (c) Kinetics of off-exchange from residues 96 to 112 of thrombin alone (■) and in complex with TMEGF45 (●) at pH 6.6. (d) The same as (c) but at pH 7.9. (e) Kinetics of off-exchange from residues 97 to 117 of thrombin alone (■) and in complex with TMEGF45 (●) at pH 6.6. (f) The same as in (e) but at pH 7.9.

Table 3. Solvent accessibility of the regions adjacent to anion-binding exosite I

A. Sequence		Mass (MH+)			
54-61		1004.55			
Sample	On by 10 min (8.6 possible) ^a		Fast off (6 amides) ^b	Intermed off	Slow off
pH 6.60 thrombin +TMEGF45	5.0		2.9 (0.34)	0	1.2 (0.27)
pH 7.90 thrombin +TMEGF45	7.6		1.9 (0.02)	0	2.2 (0.01)
			5.0 (0.22)	0	1.7 (0.17)
			4.3 (0.23)	0	2.4 (0.16)
B. Sequence		Mass (MH+)			
167-180		1506.78			
Sample	On by 10 min (14.6 possible) ^a		Fast off (13 amides) ^b	Intermed off	Slow off
pH 6.60 thrombin +TMEGF45	7.0		4.4 (0.15)	0	1.4 (0.08)
pH 7.90 thrombin +TMEGF45	10.9		3.1 (0.23)	0.7 (0.18)	2.0 (0.13)
			6.7 (0.50)	0	3.4 (0.28)
			5.1 (0.22)	0	5.1 (0.12)

All deuterium levels were corrected to account for ~40% loss during analysis.

The error to the fit for each value is indicated in parentheses.

^a The number of possible sites of deuteration = number of amides + 4.4% of all exchangeable sites (based on final dilution of sample before drying).

^b The number of backbone amides (not including the N-terminal residue).

Table 4. Solvent accessibility of the path to the active site

A. Sequence		Mass (MH+)			
139-149		1263.71			
Sample	On by 10 min (11.6 possible) ^a		Fast off (9 amides) ^b	Intermed off	Slow off
pH 6.60 thrombin +TMEGF45	7.8		5.6 (0.31)	0	1.7 (0.18)
pH 7.90 thrombin +TMEGF45	8.9		3.8 (0.23)	3.1 (1.10)	0.4 (1.25)
			6.7 (0.20)	0	1.7 (0.11)
			6.4 (0.26)	0	2.0 (0.14)
B. Sequence		Mass (MH+)			
281-293		1702.02			
Sample	On by 10 min (13.7 possible) ^a		Fast off (12 amides) ^b	Intermed off	Slow off
pH 6.60 thrombin +TMEGF45	7.1		4.8 (0.08)	0	1.5 (0.05)
pH 7.90 thrombin +TMEGF45	9.6		<0.01	5.1 (0.48)	1.6 (0.07)
			6.8 (0.30)	0	2.1 (0.17)
			4.9 (0.35)	0	4.0 (0.20)
C. Sequence		Mass (MH+)			
117-125		1168.68			
Sample	On by 10 min (8.0 possible) ^a		Fast off (7 amides) ^b	Intermed off	Slow off
pH 6.6 thrombin +TMEGF45	9.4		6.9 (0.17)	0	1.7 (0.10)
pH 7.90 thrombin +TMEGF45	8.5		6.3 (0.66)	0	2.3 (0.45)
			6.2 (0.23)	0	1.5 (0.13)
			6.8 (0.53)	0	1.0 (0.27)
D. Sequence		Mass (MH+)			
117-132		2144.14			
Sample	On by 10 min (15.9 possible) ^a		Fast off (14 amides) ^b	Intermed off	Slow off
pH 6.60 thrombin +TMEGF45	13.3		5.6 (1.20)	3.9 (1.13)	2.9 (0.15)
pH 7.90 thrombin +TMEGF45	14.9		4.6 (0.38)	4.5 (0.78)	3.2 (0.97)
			10.9 (0.53)	0	3.0 (0.35)
			8.5 (0.65)	2.3 (0.60)	3.2 (0.12)

All deuterium levels were corrected to account for ~40% loss during analysis.

The error to the fit for each value is indicated in parentheses.

^a The number of possible sites of deuteration as in Tables 2 and 3.

^b The number of backbone amides (not including the N-terminal residue).

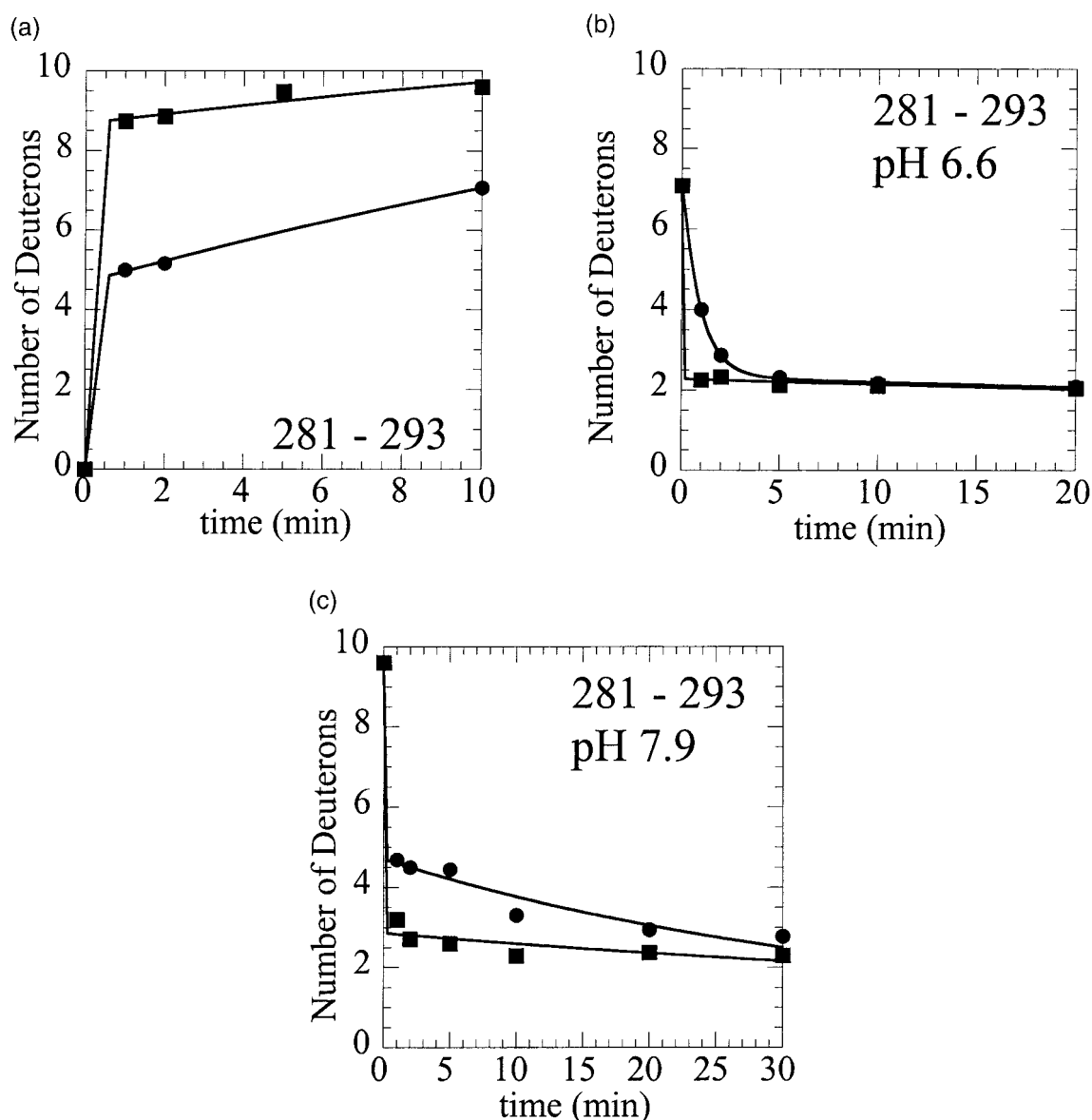


Figure 6. (a) Kinetics of deuterium incorporation into the C-terminal helix of thrombin, residues 281 to 293 (m/z 1702.02) at pH 6.6 (●) and pH 7.9 (■). (b) Kinetics of off-exchange from residues 281 to 293 of thrombin alone (■) and in complex with TMEGF45 (●) at pH 6.6. (c) as in (b) but at pH 7.9. A second related peptide of mass 2202.26 (residues 276 to 292) showed similar kinetics (data not shown).

region containing the thermodynamically most important residues for the interaction. The hot spot of the thrombin-TM interaction may be the hydrophobic pocket formed from Phe55, Tyr107, Ile114 and Leu96 that binds Ile414 of TM (Fuentes-Prior, 2000). So far, only Tyr107 has been mutated to alanine, and this mutant showed the most severe loss of TM binding of all the alanine mutants studied (Hall *et al.*, 1999). None of the other hydrophobic residues that surround our proposed hot spot (Leu54, Phe55, Leu96, Val97, Ile99 and Ile111) was selected for mutation in this alanine scanning study. Still, the drastic loss of TM binding upon mutation of Tyr107 suggests that the hot spot is also the solvent-inaccessible core of the interface. These results point to further experiments: first to mutate the other residues in the proposed hot spot

to confirm its identity, and second, to test whether the hot spot of other protein-protein interactions is also the part of the interface that is completely solvent-excluded. If so, measurement of the kinetics of amide H/²H exchange in the complex would be a much simpler way to identify the hot spot of a protein-protein interaction than alanine scanning mutagenesis.

Solvent exclusion and the thermodynamics of the thrombin-TMEGF45 interaction

While solvent exclusion at a protein-protein interface has been thought to be a consequence of tight binding, we are aware of only one other study that has directly measured solvent exclusion at a protein-protein interface. Paterson *et al.* (1991)

used NMR to measure H/²H exchange rates of amides in the horse cytochrome *c*-E8 monoclonal antibody complex. The authors were able to determine protection factors ($k_{\text{free}}/k_{\text{bound}}$) for individual amides. One amide (Arg38) of cytochrome *c* was found to be slowed by a factor of 340, which correlated with the predicted protection factor of ~300 for a completely buried amide. By comparison, the three completely solvent-excluded amides in the 96-112 region showed rate decreases from ~10 min⁻¹ in free thrombin to ~0.02 min⁻¹ in the TMEGF45 complex. This exchange rate in the complex is that predicted by equation (3) if k_{ex} was 10 min⁻¹ and values of k_a and k_d are as listed in Table 1.

Previous studies have shown that the ΔG for the thrombin-TM interaction is dominated by an increase in entropy since ΔH is ~0 at 298 K (Vindigni *et al.*, 1997). In the case of TMEGF45-thrombin, the K_d is 50 nM, so the ΔG of binding is -9.9 kcal/mol at 298 K. Since $\Delta G = \Delta H - T\Delta S$, and $\Delta H = 0$, $\Delta S = 33 \text{ cal}/(\text{mol K})^{-1}$. Reactions driven by entropy alone must overcome the entropic barrier imposed by the loss of translational and rotational degrees of freedom in the unbound state, which are partially offset by residual intermolecular motions (Brady & Sharp, 1997; Janin, 1996). One source of entropy gain is the liberation of bound water at the complex interface, and this may provide a significant portion of the energetic gain in the thrombin-TMEGF45 interaction. This hypothesis is consistent with the highly negative heat capacity change observed for this interaction (Vindigni *et al.*, 1997). Experiments have shown that the average increase in entropy upon liberation of a water molecule from the surface of a cyclic dipeptide is $2.0(\pm 1.6) \text{ cal}/(\text{mol K})^{-1}$ (Habermann & Murphy, 1996). To account for the entropy change upon binding of TMEGF45 to thrombin, about 16 water molecules would need to be liberated from interface. While the experiments performed here are not capable of explicitly determining the number of water molecules excluded from the interface, the observation of solvent-excluded amides is fully consistent with a significant release of water from the interface. It is interesting to speculate that the release of bound water is accomplished by the flexible loops of the fifth EGF-like domain of TM, which all showed chemical shift perturbations upon binding to thrombin, perhaps with the TM loops fitting into the nooks and crannies of the thrombin surface (Wood *et al.*, 2000).

Allosteric effects due to TMEGF45 binding

An allosteric mechanism for the activation of protein C by TMEGF45 is supported by numerous observations. TMEGF45 alters the k_{cat} of thrombin for protein C from 2 min⁻¹ to 250 min⁻¹ (a factor of 125), but the K_m changes by a factor of only 12, from 60 nM to 5 nM (Esmon, 1995). Fluorescent active-site labels, spin labels, and synthetic substrates have all demonstrated that conformational

changes take place near the S2 substrate-binding pocket in the thrombin active site when TM fragments containing the fourth EGF-like domain bind, but not when fragments containing only the fifth and sixth EGF-like domains bind (Ye *et al.*, 1991, 1992; Musci *et al.*, 1988). Conversely, the crystal structure of thrombin complexed to TMEGF456 with an inhibitor in the active site displays no conformational differences with respect to other crystal structures of thrombin (Fuentes-Prior *et al.*, 2000). It is possible that the thrombin-TM complex is dynamic, and that TM binding alters the distribution of conformational states of thrombin in solution, but this would not be observed in the crystal. Our results point to several possible modes of allosteric change that may be induced by binding of TMEGF45 to thrombin.

First, the tight contact between TMEGF45 and the 54-61 region of thrombin may change the conformation of Glu61 that is thought to have an unfavorable interaction with Asp residues in protein C (Erlich *et al.*, 1990; Le Bonniec *et al.*, 1991). It is likely that binding to this region as well as to the 96-112 region of thrombin induces changes in the 167-180 region, which also extends through the back side and includes Trp177 (Trp141 in chymotrypsin numbering). This tryptophan residue has also been implicated in fluorescent changes upon TM binding.

Second, slowing of amide exchange was seen for a path of amides extending along the surface of thrombin *via* the 139-149 segment and C-terminal helix to a loop immediately preceding the catalytic aspartate. Within the 139-149 segment, mutation of Lys142 to alanine significantly decreased TM binding (Lys106 in Hall *et al.*, 1999). It is interesting that we observed slowing of H/²H exchange for this region when TMEGF45 was bound to thrombin, but in the crystal structure it is the sixth domain that is contacting Lys142. The structure of TMEGF45 indicates that it is an extremely dynamic molecule, and as such, the fourth domain may make transient contacts across the face of thrombin from anion-binding exosite I to the C-terminal helix (Wood *et al.*, 2000). Tightening or pushing-up on the C-terminal helix could cause conformational changes in residues 126 to 132 that would result in the observed slowing of H/²H exchange for amides in this segment. This loop forms part of the binding site for residues at the P2 and P3 positions of the substrate. It contains Leu131, a S2 pocket residue that also forms contacts to the rest of the binding pocket that accommodates the P2 residue of the substrate causing subtle substrate specificity changes. Indeed, it was precisely when fluorescent labels were placed at the P2 position of the substrate that changes were seen when TM fragments containing the fourth domain were bound to thrombin (Ye *et al.*, 1991).

The H/²H exchange results presented here are consistent with previous studies showing allosteric effects of TM on thrombin. The observed partial solvent-inaccessibility may be due to transient

contact of the fourth domain along the surface of thrombin, or may be due to allosteric conformational changes. A good starting point to differentiate between these two may be further H/²H exchange studies on complexes of thrombin with TM mutants that are known to have altered protein C activation properties.

Materials and Methods

Proteins

TMEGF45 was expressed in *Pichia pastoris* yeast as described by White *et al.* (1995). The protein was first purified by anion-exchange chromatography (QAE Sephadex followed by HiLoad 26/10 Q Sepharose) followed by HiLoad 16/60 Superdex 75 size-exclusion chromatography (Pharmacia Biotech, Uppsala, Sweden). TMEGF45 was further purified and desalted by reverse-phase HPLC as described (Wood & Komives, 1999), and TMEGF456 was exchanged into water by centrifugation with a Centricon-10 filter (Millipore Corp., Bedford, MA, USA). Human α -thrombin was a generous gift from Dr John Fenton and was exchanged into 12.5 mM potassium phosphate buffer, 25 mM NaCl (pH 6.5), using a Centricon-10 filter. No active-site inhibitor was used. Aliquots were lyophilized and stored at -20°C until use.

Protein concentrations were determined by amino acid analysis. Lyophilized thrombin and TMEGF45 samples were hydrolyzed with 6M HCl at 110°C for 20 hours. After hydrolysis, each sample was lyophilized, dissolved in 20 mM HCl, and analyzed using a Hitachi L-8500A amino acid analyzer (Tokyo, Japan). Thrombin aliquots contained 435 picomoles of thrombin, 375 nanomoles of K_2PO_4 , and 750 nM NaCl; TMEGF45 aliquots contained 3.18 nM.

Measurement of thrombin-TMEGF45 binding kinetics

Surface plasmon resonance experiments were performed using a Biacore 3000 surface plasmon resonance instrument (Biacore, Inc., Piscataway, NJ) as described in detail elsewhere (Baerga-Ortiz *et al.*, 2000).

Mass spectrometry

Matrix-assisted laser desorption time-of-flight (MALDI-TOF) mass spectra were acquired on a Voyager DE STR (PE Biosystems, Foster City, CA, USA). Data were acquired as described elsewhere (Mandell *et al.*, 1998a). All reported masses are theoretical monoisotopic MH^+ masses unless otherwise noted. The matrix used was 5 mg/ml α -cyano-4-hydroxycinnamic acid (Sigma, St. Louis, MO, USA), in a solution containing 1:1:1 acetonitrile, ethanol, and 0.1% (v/v) TFA and was adjusted to pH 2.2 with 2% TFA using an Inlab 423 pH electrode (Mettler Toledo, Wilmington, MA, USA).

Electrospray Fourier Transform Ion Cyclotron Resonance (ESI-FTICR) Mass spectrometry was carried out on a Bruker (Billerica, MA, USA) Bio-APEX II Spectrometer equipped with a 7 T magnet and an external electrospray ion source (Analytica, Branford, CT, USA) by accumulating 128 scans per sample. The temperature of the drying gas for ESI was set to 250°C . The capillary exit potential was set to 80-100V and the trapping time was 0.5-1 second. Spectra were internally calibrated on known peptides from the thrombin digest. Samples were pre-

pared exactly as described for the MALDI and then desalted using zip tips (Millipore, Bedford, MA, USA) prior to infusion into the electrospray source.

Thrombin digestion and identification of peptic fragments

The identification of each peptide in the digest mixture was described previously (Mandell *et al.*, 1998b, 1999). The identity of most peaks was confirmed by mass searching using masses measured with a high-resolution Fourier transform ion cyclotron resonance mass spectrometer equipped with a 7 T magnet and an electrospray ionization source (Bruker Daltonics, Inc., Billerica, MA, USA). The theoretical mass of all peptides identified by FTICR was within five parts per million of the mass measured using the high-resolution instrument.

pH of H/²H exchange mixtures

pH measurements were made on non-deuterated mock solutions to avoid electrode isotope effects. The pH of small volumes ($\sim 12\ \mu\text{l}$) used during protein complexation was measured with a micro PHR-146 pH electrode (Lazar Research Laboratories, Inc., Los Angeles, CA, USA). The pH of larger volumes ($\sim 100\ \mu\text{l}$) was measured with a more accurate Inlab 423 pH electrode (Mettler Toledo, Wilmington, MA, USA). Deuterated buffer solutions were prepared from 1 M stock buffers (in H_2O) in exactly the same manner as the mock solutions.

Measurement of the rate of incorporation of deuterons into surface amides of thrombin

The number of deuterons incorporated into different regions of thrombin over ten minutes was measured in buffered $^2\text{H}_2\text{O}$ at pH 6.6 and 7.9. The kinetics of incorporation are a good measure of the solvent accessibility of each region of thrombin. The number of deuterons incorporated at ten minutes was also used as the $t = 0$ value in the off-exchange experiments described below. After incubation, samples were simultaneously quenched and diluted by addition of 120 μl of H_2O buffer (0°C) with $\sim 5\ \mu\text{l}$ of 2% TFA to give a final pH of 2.5. Each sample was then digested at 0°C for five minutes with a 1:1 molar ratio of immobilized pepsin, which was removed by centrifugation at 14,000 RPM for one minute at 4°C . Finally, the supernatant was frozen in liquid N_2 .

Frozen samples were quickly (<30 seconds) defrosted to 0°C , mixed 1:1 with 0°C matrix, and $0.5\ \mu\text{l}$ was spotted onto a chilled MALDI target. The target was immediately placed into a desiccator under a moderate vacuum such that the spot would dry in approximately one minute. Slow drying under moderate vacuum was found to improve sample analysis, presumably because of improved crystal growth. The chilled, dried plate was transferred as quickly as possible (<10 seconds) to the mass spectrometer. Samples were analyzed on individual target plates so that each sample was treated identically and experienced the same amount of artifactual back exchange, thereby avoiding the necessity of correcting for back exchange occurring during analysis (Mandell *et al.*, 1998a). About three minutes elapsed from the time of defrosting to analysis with the bulk of the time being the one minute of slow drying and the 1.5 minutes that elapses between the time the target is loaded into the spectrometer and when the first laser

shot occurs. Data were collected for 256 scans over 256 seconds (Mandell *et al.*, 1998a).

Measurement of the rates of off-exchange of deuterons from the thrombin-TMEGF45 complex

The rates of off-exchange of deuterons from thrombin in complex with TM fragments were measured as described elsewhere (Mandell *et al.*, 1998a,b). Experiments were carried out at 25 °C. Lyophilized samples of either thrombin or TM were hydrated with 6 μ l of $^2\text{H}_2\text{O}$ buffer. For experiments performed at pH 6.6, the thrombin buffer was 50 mM Tris base (pH 6.5) and the TMEGF45 buffer was 10 mM Tris base, 10 mM CaCl_2 . For experiments performed at pH 7.9, the thrombin buffer was 50 mM Tris base and the TMEGF45 buffer was 10 mM Tris base, 10 mM CaCl_2 . Thrombin and TMEGF45 samples were incubated separately in $^2\text{H}_2\text{O}$ for eight minutes before combining them (12 μ l total) and allowing them to complex for two minutes. The complex was off-exchanged for varying times (1 to 30 minutes) by 1:10 dilution with 120 μ l of H_2O buffer (10 mM Tris base, either pH 6.6 or pH 7.9, as appropriate). The pH variation of the complexation and dilution buffers was never more than ~ 0.1 unit. $\text{H}/^2\text{H}$ exchange was quenched at 0 °C to pH 2.5 by addition of 1% (for pH 6.6 experiments) or 2% (for pH 7.9 experiments) TFA (~ 6 μ l). The precise amount of TFA required for quenching was determined by titration prior to each experiment. Protein digestion and mass spectrometry analysis were performed as described above.

Control experiments were performed to determine the rates of deuteron off-exchange from thrombin in the absence of TMEGF45. To reproduce the same pH and volume conditions as for the thrombin-TM experiments, instead of adding 6 μ l of TM to thrombin after eight minutes of incubation in $^2\text{H}_2\text{O}$, 6 μ l of 10 mM Tris base 10 mM CaCl_2 , pH 8.0 was added for experiments at both pH values. The pH of the dilution buffer for samples containing thrombin alone and samples of thrombin with TMEGF45 were within 0.15 unit of each other. Because the off-exchange was accomplished by dilution of the 100% $^2\text{H}_2\text{O}$ solution to $\sim 10\%$, a fraction of exchangeable deuterons was always observed and appeared to be off-exchanging slowly as the number equilibrated against the residual $^2\text{H}_2\text{O}$.

Data analysis

Mass spectra were calibrated using the theoretical mass of two prominent previously identified thrombin peptides (1048.5328 and 2144.1406). For some deuterated samples the monoisotopic peak was not present, so higher mass peaks of the same envelope were used; these peaks were identified based upon the internal calibration of the mass spectrometer. The average mass of a peptide was calculated by determining the centroid of its isotopic envelope as described by Mandell *et al.* (1998a). The difference between the average masses of the deuterated and non-deuterated peptide gave the number of deuterons incorporated. To correct for back exchange during analysis, a factor of 1.667 was applied (Mandell *et al.*, 1998a) based on previous observations that the number of deuterons was approximately 60% of the total possible.

Kinetic plots of deuteration of thrombin amides fit best to a two-exponential model accounting for deuterons exchanging at a very rapid rate (fully solvent-

accessible amides) and an intermediate rate (amides with reduced solvent-accessibility in the folded protein) using the following equation:

$$D = N_{\text{fast}}(1 - e^{-k_{\text{fast}}t}) + N_{\text{slow}}(1 - e^{-k_{\text{slow}}t})$$

where D is the total number of deuterons at time, t , N_{fast} is the number of deuterons exchanging at the fast rate, k_{fast} and N_{slow} is the number of deuterons exchanging at the slow rate, k_{slow} . The fit was implemented in Kaleidagraph 3.0 (Synergy Software, Inc.). The rapidly exchanging protons had all exchanged by the first time-point, so k_{fast} was fixed. Other floating parameters (N_{fast} , N_{slow} and k_{slow}) were completely insensitive to changes in the value of k_{fast} from 10 min^{-1} to 100 min^{-1} , so k_{fast} was set to 30 min^{-1} , the median of the amide exchange rates for the rapidly exchanging amides in the mannose permease domain P13 from *E. coli* (Gemmecker *et al.*, 1993).

Kinetics of off-exchange of deuterons from thrombin amides fit best to either a bi or tri-exponential model. The different rates reflect those amides that were not protected from solvent in the complex and remained fast exchanging (set to 30 min^{-1}), those partially excluded and exchanging at an intermediate rate (typically 0.1 to 0.5 min^{-1}), and those completely excluded that exchange at a slow rate (typically 0.04 to < 0.01 min^{-1}). The bi-exponential model was used when no improvement in the fit was observed when the bi and tri-exponential models were compared. In these cases, typically no deuterons were found to exchange at the intermediate rate. The tri-exponential equation is:

$$D = N_{\text{fast}}e^{-k_{\text{fast}}t} + N_{\text{inter}}e^{-k_{\text{inter}}t} + N_{\text{slow}}e^{-k_{\text{slow}}t} + 0.044(P)$$

where D represents the number of deuterons at time t , N_{fast} represents the number of fast-exchanging deuterons, k_{fast} is the fast-exchange rate, N_{inter} is the number of intermediate-exchanging deuterons, k_{inter} is the intermediate-exchange rate, N_{slow} is the number of slow-exchanging deuterons, k_{slow} is the slow-exchange rate. The fast rate k_{fast} was again fixed at 30 min^{-1} and the other variables were not sensitive to this fast rate. The value of 0.044 (P) accounts for the residual deuteration of all exchangeable protons on the peptide (including side-chains) after all dilutions into protonated solutions are made prior to drying on the MALDI target plate. This residual amount of deuterium, proportional to the number of exchangeable sites, was still observed on each peptide at infinite time.

Acknowledgments

This work was supported by NSF MCB-9808286 and NIH HL47463 to E.A.K. J.G.M. received support from T32-CA09 and the Burroughs-Wellcome Fund. A.B.O. received support from NIH F31.H 10095.

References

- Baerga-Ortiz, A., Rezaie, A. R. & Komives, E. A. (2000). Electrostatic dependence of the thrombin-thrombomodulin interaction. *J. Mol. Biol.* **296**, 651-658.
- Bai, Y. W., Milne, J. S., Mayne, L. & Englander, S. W. (1993). Primary structure effects on peptide group hydrogen exchange. *Proteins: Struct. Funct. Genet.* **17**, 75-86.

- Brady, G. P. & Sharp, K. A. (1997). Entropy in protein folding and in protein-protein interactions. *Curr. Opin. Struct. Biol.* **7**, 215-221.
- Cunningham, B. C. & Wells, J. A. (1993). Comparison of a structural and a functional epitope. *J. Mol. Biol.* **234**, 554-563.
- Dharmasiri, K. & Smith, D. L. (1996). Mass spectrometric determination of isotopic exchange rates of amide hydrogens located on the surfaces of proteins. *Anal. Chem.* **68**, 2340-2344.
- Erlich, H. J., Grinnell, B. W., Jaskunas, S. R., Esmon, C. T., Yan, S. B. & Bang, N. U. (1990). Recombinant human protein C derivatives: altered response to calcium resulting in enhanced activation by thrombin. *EMBO J.* **9**, 2367-2373.
- Esmon, C. T. (2000). Regulation of blood coagulation. *Biochim. Biophys. Acta*, **1477**, 349-360.
- Fuentes-Prior, P., Iwanaga, Y., Huber, R., Pagila, R., Rumennik, G., Seto, M., Morser, J., Light, D. R. & Bode, W. (2000). Structural basis for the anticoagulant activity of the thrombin-thrombomodulin complex. *Nature*, **404**, 518-525.
- Gemmecker, G., Jahnke, W. & Kessler, H. (1993). Measurement of fast proton exchange rates in isotopically labeled compounds. *J. Am. Chem. Soc.* **115**, 11620-11621.
- Habermann, S. M. & Murphy, K. P. (1996). Energetics of hydrogen bonding in proteins: a model compound study. *Protein Sci.* **5**, 1229-1239.
- Hall, S. W., Nagashima, M., Zhao, L., Morser, J. & Leung, L. (1999). Thrombin interacts with thrombomodulin, protein C, and thrombin-activatable fibrinolysis inhibitor *via* specific and distinct domains. *J. Biol. Chem.* **274**, 25510-25516.
- Herberg, F. W., Doyle, M. L., Cox, S. & Taylor, S. S. (1999). Dissection of the nucleotide and metal-phosphate binding sites in cAMP-dependent protein kinase. *Biochemistry*, **38**, 6352-6360.
- Hvidt, A. & Nielsen, S. O. (1966). Hydrogen exchange in proteins. *Advan. Protein Chem.* **21**, 287-386.
- Janin, J. (1996). Quantifying biological specificity: the statistical mechanics of molecular recognition. *Proteins: Struct. Funct. Genet.* **25**, 438-445.
- Le Bonniec, B. F., Macgillivray, R. T. A. & Esmon, C. T. (1991b). Thrombin Glu-39 restricts the P3 specificity to nonacidic residues. *J. Biol. Chem.* **266**, 13796-13803.
- Lo Conte, L., Chothia, C. & Janin, J. (1999). The atomic structure of protein-protein recognition sites. *J. Mol. Biol.* **285**, 2177-2198.
- Mandell, J. G., Falick, A. M. & Komives, E. A. (1998a). Measurement of amide hydrogen exchange by MALDI-TOF mass spectrometry. *Anal. Chem.* **70**, 3987-3995.
- Mandell, J. G., Falick, A. M. & Komives, E. A. (1998b). Identification of protein-protein interfaces by decreased amide proton solvent accessibility. *Proc. Natl Acad. Sci. USA*, **95**, 14705-14710.
- Mandell, J. G., Falick, A. M. & Komives, E. A. (1999). Identification of protein-protein interfaces by amide proton exchange coupled to MALDI-TOF mass spectrometry. In *Mass Spectrometry in Biology and Medicine* (Burlingame, A. L., ed.), pp. 91-109, Humana Press, Totowa, NJ.
- Musci, G., Berliner, L. J. & Esmon, C. T. (1988). Evidence for multiple conformational changes in the active center of thrombin induced by complex formation with thrombomodulin: an analysis employing nitroxide spin-labels. *Biochemistry*, **27**, 769-773.
- Myszka, D. G., Arulanantham, P. R., Sana, T., Wu, Z., Morton, T. A. & Ciardelli, T. L. (1996). Kinetic analysis of ligand binding to interleukin-2 receptor complexes created on an optical biosensor surface. *Protein Sci.* **5**, 2468-2478.
- Nicholls, A., Sharp, K. A. & Honig, B. (1991). Protein folding and association: insights from the interfacial and thermodynamic properties of hydrocarbons. *Proteins: Struct. Funct. Genet.* **11**, 281-296.
- Paterson, Y., Englander, S. W. & Roder, H. (1990). An antibody binding site on cytochrome c defined by hydrogen exchange and two-dimensional NMR. *Science*, **249**, 755-759.
- Vindigni, A., White, C. E., Komives, E. A. & Di Cera, E. (1997). Energetics of thrombin-thrombomodulin interaction. *Biochemistry*, **36**, 6674-6681.
- Wells, J. A. (1996). Binding in the growth hormone receptor complex. *Proc. Natl Acad. Sci. USA*, **93**, 1-6.
- White, C. E., Hunter, M. J., Meininger, D. P., White, L. R. & Komives, E. A. (1995). Large-scale expression, purification and characterization of small fragments of thrombomodulin: the roles of the sixth domain and of methionine 388. *Protein Eng.* **8**, 1177-1187.
- Wood, M. J. & Komives, E. A. (1999). Production of large quantities of isotopically labeled protein in *Pichia pastoris* by fermentation. *J. Biomol. NMR*, **13**, 149-159.
- Wood, M. J., Sampoli, B. & Komives, E. A. (2000). Solution structure of the smallest cofactor-active fragment of thrombomodulin. *Nature Struct. Biol.* **7**, 200-204.
- Wu, H., Myszkka, D. G., Tendian, S. W., Brouillette, C. G., Sweet, R. W., Chaiken, I. M. & Hendrickson, W. A. (1996). Kinetic and structural analysis of mutant CD4 receptors that are defective in HIV gp120 binding. *Proc. Natl Acad. Sci. USA*, **93**, 15030-15035.
- Ye, J., Esmon, N. L., Esmon, C. T. & Johnson, A. E. (1991). The active site of thrombin is altered upon binding to thrombomodulin. Two distinct structural changes are detected by fluorescence, but only one correlates with protein C activation. *J. Biol. Chem.* **266**, 23016-23021.
- Ye, J., Liu, L. W., Esmon, C. T. & Johnson, A. E. (1992). The fifth and sixth growth factor-like domains of thrombomodulin bind to the anion-binding exosite of thrombin and alter its specificity. *J. Biol. Chem.* **267**, 11023-11028.

Edited by M. F. Moody

(Received 16 August 2000; received in revised form 21 November 2000; accepted 27 November 2000)